Journal of Neurochemistry

JOURNAL OF NEUROCHEMISTRY | 2017 | 143 | 244–256 doi: 10.1111/jnc.14154

ORIGINAL ARTICLE

Mst-1 deficiency promotes post-traumatic spinal motor neuron survival via enhancement of autophagy flux

Mengting Zhang,* Wufan Tao,† Zengqiang Yuan‡ and Yaobo Liu*

*Institute of Neuroscience, Jiangsu Key Laboratory of Translational Research and Therapy for Neuro-Psycho-Diseases, Soochow University, Suzhou, China

†Obstetrics & Gynecology Hospital and Institute of Developmental Biology and Molecular Medicine, Collaborative Innovation Center of Genetics and Development, School of Life Sciences, Fudan University, Shanghai, China

‡Brain Science Center at the Institute of Basic Medical Science, Haidian District, Beijing, China

Abstract

The mammalian Ste20-like kinase 1 (Mst-1) is a serine-threonine kinase and a component of the Hippo tumor suppressor pathway, which reacts to pathologically relevant stress and regulates cell death. However, little is known about its role in spinal cord injury. Here, we found that p-Mst-1, the activated form of Mst-1, was induced in the post-traumatic spinal motor neurons. *In vivo* evidence demonstrated that Mst-1 deficiency promoted post-traumatic spinal motor neuron survival, Basso mouse scale scores, and synapse survival. Moreover, we found that autophagosome formation and autolysosome degradation enhanced by Mst-1 deficiency were crucial to attenuate the death of injured spinal motor neurons. Taken together, our findings demonstrate that Mst-1 deficiency promotes post-traumatic spinal motor neuron survival via enhancement of autophagy flux.

Keywords: autolysosome degradation, autophagy, hippo signaling, Mst-1, neuroprotection, spinal cord injury.

J. Neurochem. (2017) **143**, 244–256.

Spinal cord injury is a devastating condition causing paralysis and sensorimotor impairments, which consists of primary and secondary injury and their mechanisms has not been clearly stated yet (Zou 2013). The primary injury occurs simultaneously at the accident, leading to neuron death directly; whereas, the secondary injury is characterized by extensive and persistent pathological stress, including ischemia, oxidative stress, ionic homeostasis disturbances, and inflammatory responses. Finally, the overloaded pathological stress results in worse neuron viability around the primary lesion site, further resulting in locomotor dysfunction and retarded post-traumatic recovery. Although we cannot avoid the accident if it has happened and the primary injury afterward, what we can do is to save more neurons during secondary injury. Based on this context, although the exact molecular pathway of the secondary injury still remains elusive, removal of these deleterious stress response factors during secondary injury might promote post-traumatic spinal neuron survival (Cordaro *et al.* 2016; Li *et al.* 2016; Zhang *et al.* 2016).

Autophagy is a cell survival-promoting pathway, in which autophagosomes allow autophagy to remove damaged organelles and protein aggregates, and maintain organelle function and protein quality. Autophagy is initiated by the

Received March 19, 2017; revised manuscript received July 20, 2017; accepted August 14, 2017.

Address correspondence and reprint requests to Dr Yaobo Liu, Institute of Neuroscience, Jiangsu Key Laboratory of Translational Research and Therapy for Neuro-Psycho-Diseases, Soochow University, Suzhou, China. E-mail: liuyaobo@suda.edu.cn

Abbreviations used: ALS, amyotrophic lateral sclerosis; Baf, bafilomycin A1; BMS, Basso mouse scale; ChAT, choline acetyltransferase; DAPI, 4′-6-Diamidino-2-phenylindole; ER, endoplasmic reticulum; FG, fluorogold; GAPDH, glyceraldehyde-3-phosphate dehydrogenase; GFAP, glial fibrillary acidic protein; HRP, horseradish peroxidase; i.p., intraperitoneally; LC3, light chain 3; LSD, least significant differences post-test; Mst-1, mammalian Ste20-like kinase 1; NeuN, neuron-specific nuclear-binding protein; p62/SQSTM1, sequestosome-1; PBS, phosphate-buffered saline; PFA, paraformaldehyde; p-Mst-1, phosphorylated Mst-1; RIPA, radioimmunoprecipitation assay; ROS, reactive oxygen species; SCI, spinal cord injury; vGlut1, vesicular glutamate transporter 1.

© 2017 International Society for Neurochemistry,

formation of double-membraned autophagosomes which encapsulate toxic protein and cytoplasm, then autophagosomes and lysosomes fuse together leading to their toxic content degradation. This total progress is also termed autophagy flux which plays a significant role in cellular homeostasis. However, down-regulation of autophagy below physiological level progressively leads to the intracellular accumulation of abnormal proteins, which induces various neurodegenerative disorders, such as Parkinson's disease and Alzheimer's disease. On the contrary, up-regulation of autophagy is generally compensatory, resulting in energy loss alleviation, damaged organelle and protein aggregate scavenging, which is also involved in the pathology of spinal cord injury (SCI) (Ravikumar *et al.* 2004; Sekiguchi *et al.* 2012). However, some studies indicated that enhanced autophagy leads to more neuron death (Kanno *et al.* 2011), and some other studies stated that autophagy enhancement protects injured neuron survival after SCI (Zhang *et al.* 2013; Tang *et al.* 2014; Goldshmit *et al.* 2015). In addition, deregulated autophagy can cause excessive degradation of proteins and organelles and eventually cell death (Smith *et al.* 2011; Viscomi and Molinari 2014; Lipinski *et al.* 2015). In summary, autophagy is a delicate balance between neuron survival and neuron death under stress response, and the mechanism of autophagy in SCI is complicated that further needs to be elucidated.

The mammalian Ste20-like kinase 1 (Mst-1) is a serine-threonine kinase and a component of Hippo tumor suppressor pathway, which reacts to pathologically relevant stress and regulates cell death (Lehtinen *et al.* 2006; Yuan *et al.* 2009). In a previous study, Lee *et al.* (2013) showed that activated Mst-1 up-regulated in the motor neurons of amyotrophic lateral sclerosis, and genetic deficiency of Mst-1 not only delayed symptom onset and mortality, but also improved the viability of spinal motor neurons, implicating that Mst-1 may function as a key modulator of neurodegeneration. Recently, Maejima *et al.* (2013) showed that Mst-1 inhibits autophagy and promotes cell death after myocardial infarction, suggesting a key determinant for Mst-1 deficiency in enhancing autophagy flux and promoting cell survival during detrimental stress response. However, little is known about its role in SCI. Inspired by these findings, we carried out a study to investigate whether Mst-1 deficiency could enhance autophagy flux and attenuate spinal neuron death after SCI.

Materials and methods

Animals and surgeries

All animal procedures were approved by Soochow University guidelines for care and use of experimental animals. Mst-$1^{-/-}$ mice on a 129/Sv genetic background were kindly provided by Dr Wufan Tao (Fudan University, Shanghai, China) and has been previously described (Dong *et al.* 2009). All mice were raised in a density of five mice per cage in the specific pathogen-free animal facility, with 12-h light/dark cycle at controlled temperature (20–26 degree) and humidity (40–70%) with free access to food and water. A total of 416 female mice including wild-type C57/BL6J, Mst-$1^{+/+}$, and Mst-$1^{-/-}$ mice were randomly assigned into four groups: (i) Sham group, (ii) SCI group, (iii) Vehicle group (Veh), (iiii) Bafilomycin treatment group (Baf) using a completely randomized digital table. Observers were blinded to the grouping and experimental design during data collection and analysis. The exact sample size in each group is described in detail in the figure legends.

Mice were subjected to surgery at the age of 8–10 weeks (20–25 g). Firstly, mice were anesthetized with pentobarbital (40 mg/kg, i.p.), and then spinal T9 complete transection was performed as previously described (Liu *et al.* 2008; Huang *et al.* 2016). To ensure a complete transection injury, the spinal cord was transected bilaterally across the entire width and depth with iridectomy micro-scissors, followed with a micro-knife tracing the cord, pressing against the lateral and ventral sides of the vertebral cavity for completeness of the lesion, then muscle, fascia, and skin were sewn up. Urination was performed twice a day manually until bladder function regained. Surgeries were performed by an independent surgeon who was blinded to the group allocation.

Immunoblotting

To perform western blot analysis, mice were killed at day 1, day 3, week 1, week 2, week 3, and week 4 post-injury (each independent experiment includes three mice per group). A 1.5 mm spinal cord with lesion scar in the center was collected in each mouse. Then, these samples were briefly sonicated and lysed in radioimmunoprecipitation assay buffer (50 mM Tris-HCl, 150 mM NaCl, 1% NP-40, 1 mM Na2-EDTA, 0.25% Na-deoxycholate) which contained protease and phosphatase inhibitor cocktails (Roche Molecular Biochemicals, Indianapolis, IN, USA). After pretreatment, equal amounts of proteins were subjected to sodium dodecyl sulfate–polyacrylamide gel electrophoresis and transferred to polyvinylidene difluoride membranes (0.2 μm, Millipore Corporation, Bedford, MA, USA). Next, blots were incubated overnight at 4°C with primary antibodies (Mst-1, Cell Signaling Technology, Beverly, MA, USA, #3682s, RRID: AB_10694384, 1 : 1000; p-Mst-1, Sigma, St Louis, MO, USA, SAB4504042, RRID: AB_2665403, 1 : 1000; light chain 3 (LC3B), Novus Biologicals, Littleton, CO, USA, NB100-2220, RRID: AB_10003146, 1 : 1000; p62, Sigma, P0067, RRID: AB_1841064, 1 : 1000; GAPDH, Sigma, G9545, RRID: AB_796208, 1 : 1000) and then incubated with horseradish peroxidase-conjugated secondary antibodies (GE Healthcare, Pittsburgh, PA, USA). Ultimately, bands were visualized with an enhanced chemiluminescence reagent (Millipore). A researcher who was blinded to the group allocation analyzed these bands using Image J (NIH) software to obtain the intensity of signals.

Immunohistochemistry

Mice were firstly anesthetized with pentobarbital (40 mg/kg, i.p.) and perfused with normal saline, and then with 0.1 M phosphate-buffered saline which contains 4% paraformaldehyde (pH = 7.4). Spinal cord segments were transferred to 20% sucrose for 12 h and 30% sucrose for another 12 h after post-fixed with 4% paraformaldehyde overnight at 4°C, and then embedded in OCT compound

(Tissue Tek, Torrance, CA, USA). Then the tissues were sliced into coronal sections (25 μm) and incubated overnight at 4°C with primary antibodies (Mst-1, Cell Signaling Technology, #3682s, RRID: AB_10694384, 1 : 500; p-Mst-1, Sigma, SAB4504042, RRID: AB_2665403, 1 : 500; ChAT, AB144, Millipore, RRID: AB_90650, 1 : 200; neuron-specific nuclear-binding protein, Millipore, ABN78, RRID: AB_10807945, 1 : 500; GFAP-Cy3, Abcam, Cambridge, MA, USA, ab49874, RRID: AB_880203, 1 : 1000; vesicular glutamate transporter 1, Millipore, AB5905, RRID: AB_2301751, 1 : 500; LC3B, Novus, NB100-2220, RRID: AB_10003146, 1 : 500; p62, Sigma, P0067, RRID: AB_1841064, 1 : 500), and then incubated with Alexa 488- and 555- conjugated secondary antibodies (Invitrogen, Carlsbad, CA, USA, 1 : 1000) overnight at 4°C. Eventually, sections were observed under a Zeiss LSM700 confocal microscope (Zeiss, Oberkochen, Germany), and Image J (NIH) software was used for quantification. Researchers were blinded to the group allocation in these procedures.

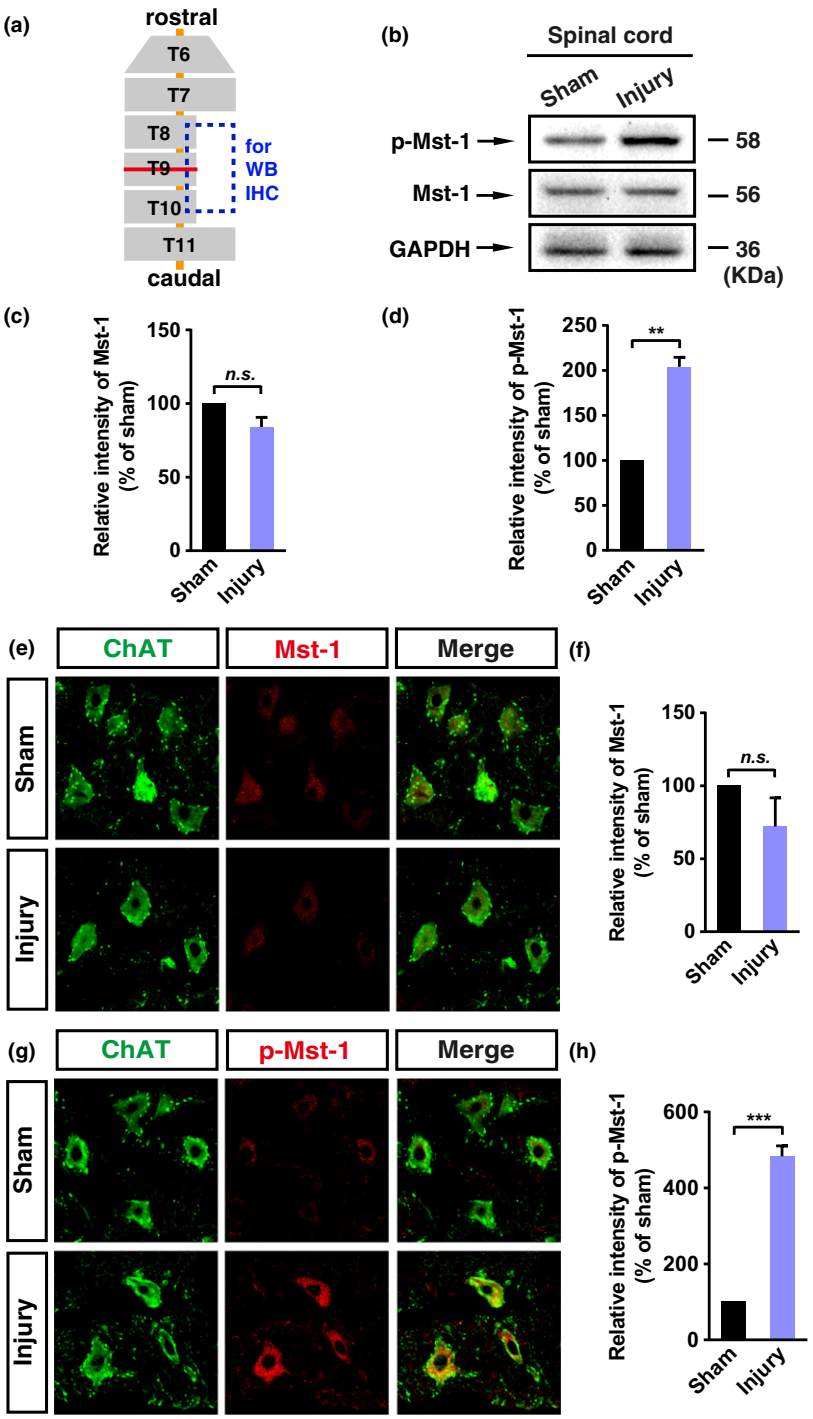

Fig. 1 Induced expression of p-Mst-1 in motor neurons at the lesion site after spinal cord injury (SCI). (a) Diagram showing that the 1.5 mm spinal cords were collected from T8 to T10 for western blot analysis and immunostaining, while the complete transection lesion site was at T9. (b–d) Western blot analysis (b) and quantification of Mst-1 (c) and p-Mst-1 (d) expression in the sham-operated and 4 weeks post-injury wild-type groups. Data were presented as mean ± SEM of three independent experiments, each independent experiment including three mice per group. Mst-1 intensity: $p = 0.1327$, *n.s.*, not significant; p-Mst-1 intensity: $p = 0.00997$, $^{**}p < 0.01$, Student's *t* test. (e and f) Co-immunostaining (e) and quantification (f) of Mst-1 and ChAT on coronal sections in the sham-operated and 4 weeks post-injury wild-type groups. Quantitative fluorescence intensity of Mst-1 was presented as mean ± SEM of more than 125 motor neurons from five independent experiments, each independent experiment including one mice per group. $p = 0.128$, *n.s.*, not significant, Student's *t* test. Scale bar, 20 μm. (g and h) Co-immunostaining (g) and quantification (h) of p-Mst-1 and ChAT on coronal sections in the sham-operated and 4 weeks post-injury wild-type groups. Quantitative fluorescence intensity of p-Mst-1 was presented as mean ± SEM of more than 125 motor neurons from five independent experiments, each independent experiment including one mice per group. $p = 0.0002$, $^{***}p < 0.001$, Student's *t* test. Scale bar, 20 μm.

Fluorogold (FG) retrograde labeling

To label motor neurons in spinal cord, a total volume of 2.4 μL fluorogold (FG) (Biotuim, Hayward, CA, USA) was injected into the longissimus, rectus abdominis, external and internal obliques of each mouse (Watson *et al.* 2009), 0.1 μL FG per injection. Then, the mice were raised for 1 more week to allow retrograde labeling the motor neurons before being killed.

Pharmacological treatments

Firstly, mice in the Bafilomycin A1 (Baf, Cayman) treatment group were intraperitoneally (i.p.) injected with Baf (10 mg/kg) 4 h after spinal T9 complete transection (Yuan *et al.* 2015), then an extra 10 μL Baf was injected in the lesion site, while the vehicle group were injected with the equivalent volume of saline. Each group of animals were injected once daily for 7 days.

Behavioral analysis

The Basso mouse scale (BMS) open-field locomotion rating scale was assessed weekly from day 1 to week 9 post-injury to analyze the function recovery of mice as previously described (Michele Basso *et al.* 2006). Four mice were excluded from the analysis because mice's hind limbs were bit and injured by themselves after SCI surgery was performed. The mice were independently evaluated by two researchers who were blinded to the group allocation. When the BMS scores of the right and left hind limbs were different, the average of the two scores was taken.

Quantification of survived motor neurons and fluorescence intensity

To analyze the number of survived motor neurons in Mst-$1^{+/+}$ and Mst-$1^{-/-}$ mice after SCI, a segment of spinal cord was cut into 25 μm serial coronal sections ranging from rostral (−600 μm) to caudal (+600 μm) around the epicenter. As the thickness of the sections were 25 μm, we may infer that there were eight sections within 200 μm range. Thus, the distance of sections around the epicenter could be confirmed by its ranking order. Moreover, the worst injured section of a spinal cord was chosen as the epicenter. In this condition, we compared the number of motor neurons in several position points, such as ± 600 μm, ± 400 μm, ± 200 μm, ± 0 μm, and the epicenter. To avoid man-made variance, only two sections closest to these points were included in the statistics. The number of motor neurons were counted with Image J by a researcher who was blinded to the group allocation, and the average of the two sections were taken as the number of motor neurons in one position.

After immunostaining, the fluorescence intensities of Mst-1, p-Mst-1, LC3, and p62 were measured with Image J. In order to avoid staining variability among sections and experimental groups, sections were incubated with the appropriate primary and secondary antibodies at the same time. Sections were observed blindly under confocal microscope, and the parameters for image capture were set from the control group and remained constant for all remaining image capturing. Data collection for densitometry was done by a researcher who was blinded to the group allocation. Five sections were randomly selected from rostral (−600 μm) to caudal (+600 μm) around the epicenter per mouse, and the intensities of more than 125 motor neurons from at least 5 independent experiments in each group were quantified.

Statistical analysis

Researchers were blinded to the group allocation in all quantification procedures. Because of the small sample sizes, assumptions of how well normality and equal variances fit the data could not be reliably assessed. Sample size was not predetermined by formal power analysis statistical methods. No samples or data were excluded from the analysis, except for four mice evaluated by BMS scores. The sample number for each experiment is stated in the figure legends. Data are presented as mean ± SEM, using Graphpad Prism 6. Quantification was used to evaluate western blot intensity, fluorescence intensity, cell number, and synapse reformation. The Student's *t* test was used for the single comparison between two groups, while the other data were analyzed with one-way ANOVA followed by Bonferroni's post-test or two-way ANOVA followed by Fisher's least significant differences post-test. $*p < 0.05$, $**p < 0.01$, $***p < 0.001$ or no significant difference (*n.s.*) denote the significance thresholds.

Results

Mst-1 shows higher activity in spinal motor neurons after SCI

To assess if Mst-1 was induced in SCI, we examined Mst-1 and the activation form of Mst-1 (p-Mst-1) in the spinal cords of intact or injured wild-type mice. Spinal T9 complete transection was performed by the previously described method (Fig. 1a). We initially assessed the expression pattern of Mst-1 and p-Mst-1 using western blot analysis (Fig. 1b). As the results show, no significant differences in total Mst-1 expression were detected in the injured group compared with the intact group (Fig. 1c). However, the activated form of Mst-1 (p-Mst-1) was strongly up-regulated in the injured group compared with the intact group (Fig. 1d). Furthermore, the co-immunostaining of Mst-1 and p-Mst-1 with choline acetyltransferase (ChAT) in the lesion area indicated that the activated form of Mst-1 (p-Mst-1) was specifically activated in spinal motor neurons after SCI (Fig. 1e–h and Figure S1a). Collectively, these data demonstrated that Mst-1 was activated in SCI, and the activation was specific for motor neurons.

Mst-1 deficiency promotes spinal motor neuron survival after SCI

To investigate whether Mst-1 deficiency was associated with the survival of spinal motor neurons after SCI, the number of survived motor neurons was analyzed by neuron-specific nuclear-binding protein, ChAT immunostaining, and FG retrograde labeling. Spinal cords were collected and cut into serial coronal sections ranging from rostral 600 μm (−600 μm) to caudal 600 μm (+600 μm) around the epicenter (Fig. 2a and b). Immunostaining results showed that homozygous deletion of Mst-1 increased the number of spinal motor neurons instead of the number of other types of spinal neurons after SCI, which implicated that Mst-1 deficiency specifically promoted the survival of post-

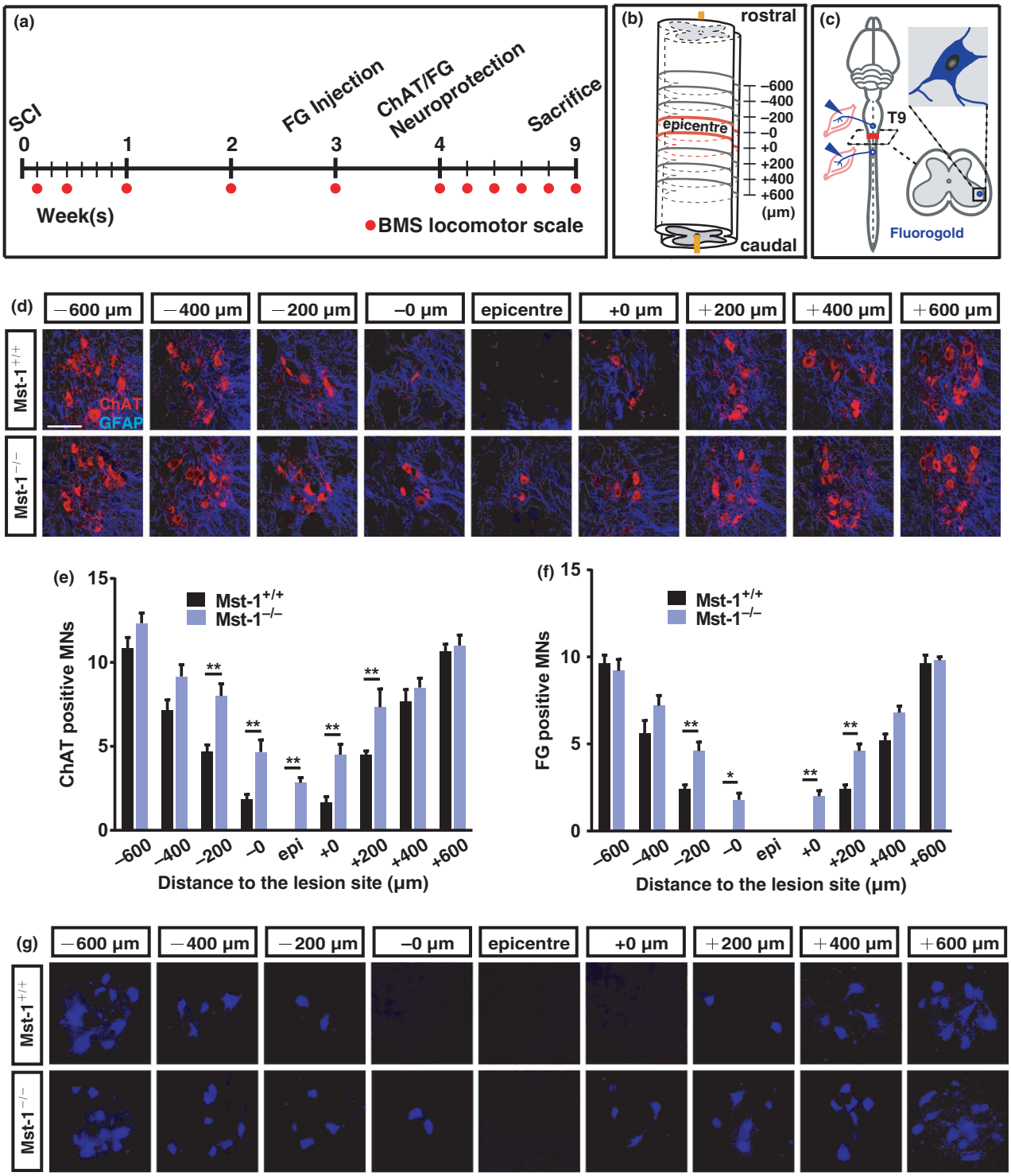

traumatic spinal motor neurons (Fig. 2d–e and Figure S1b). This result was confirmed in a contusive injury model as well (Figure S2). Moreover, FG was injected into the longissimus, rectus abdominis, external and internal obliques around the lesion site to retrogradely label spinal motor neurons, and verify whether the survived motor neurons still have connection with its innervated effector muscles in Mst-$1^{+/+}$ and Mst-$1^{-/-}$ mice (Fig. 2c). Data showed that more FG-positive neurons were detected in Mst-$1^{-/-}$ mice than in Mst-$1^{+/+}$ mice (Fig. 2f and g). These results not only

Fig. 2 Mst-1 deficiency promotes injured motor neuron survival after spinal cord injury (SCI). (a) Diagram showing the timeline of surgery performance, fluorogold (FG) tracing methods, ChAT immunostaining, and Basso mouse scale (BMS) evaluation after SCI. (b) Representative image of serial coronal sections to detect the number of ChAT or FG-positive motor neurons, ranging from rostral 600 μm (−600 μm) to caudal 600 μm (+600 μm) around the epicenter. (c) FG was injected into the thoracic muscles to retrogradely label spinal motor neurons around the lesion site after SCI. (d and e) Co-immunostaining (d) of ChAT and glial fibrillary acidic protein (GFAP) ranging from rostral 600 μm to caudal 600 μm around the epicenter in Mst-$1^{+/+}$ and Mst-$1^{-/-}$ groups 4 weeks post-injury. The number of ChAT-positive motor neurons was counted, and data were presented as mean ± SEM of six independent experiments, each independent experiment including one mice per group (e). −200 μm: $t = 4.013$, $p = 0.0011$; −0 μm: $t = 3.411$, $p = 0.0087$; epi: $t = 3.451$, $p = 0.0076$; +0 μm: $t = 3.407$, $p = 0.0088$; +200 μm: $t = 3.383$, $p = 0.0095$. $^{**}p < 0.01$, two-way ANOVA followed by Fisher's least significant differences post-test (LSD). Scale bar, 100 μm. (f and g) FG was injected into the thoracic muscles to retrogradely label spinal motor neurons ranging from rostral 600 μm to caudal 600 μm around the epicenter in Mst-$1^{+/+}$ and Mst-$1^{-/-}$ groups 4 weeks post-injury (g). The number of FG-positive motor neurons was counted, and data were presented as mean ± SEM of five independent experiments, each independent experiment including one mice per group (f). −200 μm: $t = 3.806$, $p = 0.0026$; −0 μm: $t = 3.139$, $p = 0.0219$; +0 μm: $t = 3.487$, $p = 0.0075$; +200: $t = 3.836$, $p = 0.0024$. $^{*}p < 0.05$ and $^{**}p < 0.01$, two-way ANOVA followed by Fisher's LSD. Scale bar, 100 μm.

demonstrated that Mst-1 deficiency promoted the survival of post-traumatic spinal motor neurons, but also indicated that these motor neurons have intact connection with its innervated effector muscles which might lead to better locomotor function.

Mst-1 deficiency improves BMS scores and promotes synapses survival in injured spinal cord

Open-field locomotor function of Mst-$1^{+/+}$ and Mst-$1^{-/-}$ mice which underwent T9 complete transection was measured with a well-established double-blinded analysis, the BMS scoring. In both Mst-$1^{+/+}$ and Mst-$1^{-/-}$ mice, hind limb locomotion was severely impaired for the first day post-injury, then slightly improved over time. Notably, Mst-$1^{-/-}$ mice showed higher BMS scores than Mst-$1^{+/+}$ mice at the time point of 42, 49, 56 and 63 days post-injury (Fig. 3a).

As we showed previously, Mst-1 deficiency promoted post-traumatic spinal motor neuron survival, and these survived motor neurons have intact connection with their innervated effector muscles. Thus, we assumed that there were more synapse survival in the spinal cord so that it might, at least in part, explain the higher BMS scores in Mst-$1^{-/-}$ mice (Fig. 3d). Hence, a co-immunostaining of vesicular glutamate transporter 1 and ChAT was carried out in both Mst-$1^{+/+}$ and Mst-$1^{-/-}$ mice 9 weeks post-injury to confirm the number of glutamatergic synapse. This evidence demonstrated that glutamatergic interneurons formed more glutamatergic synapses with ChAT-positive motor neurons in Mst-$1^{-/-}$ mice compared with Mst-$1^{+/+}$ mice (Fig. 3b and c).

These results revealed a detectable improvement in BMS scores in Mst-$1^{-/-}$ mice, which might be owing to more motor neuron and glutamatergic synapse survival after SCI.

Mst-1 deficiency promotes autophagy flux after SCI

Mst-1 deficiency induces autophagy and promotes cardiomyocytes survival in myocardial infarction (Maejima *et al.* 2013). Based on this report, we assumed whether Mst-1 deficiency plays a role in promoting post-traumatic spinal motor neuron survival through the enhancement of autophagy flux. To test this, we examined the expression of LC3-II, which represented the level of autophagosome formation. Firstly, from the day 1 to week 4 post-injury, up-regulation of LC3-II was detected in both Mst-$1^{+/+}$ and Mst-$1^{-/-}$ groups, while the Mst-$1^{-/-}$ group showed higher LC3-II expression than Mst-$1^{+/+}$ group at the same time points (Fig. 4a and b). In addition, this up-regulation reached a peak on the day 7 post-injury and gradually decreased until at least 4 weeks post-injury (Fig. 4c). These results demonstrated that autophagy was induced after SCI, and Mst-1 deficiency enhanced the expression of LC3-II, suggesting that endogenous Mst-1 might inhibit autophagy.

As we showed previously, Mst-1 deficiency enhanced the expression of LC3-II which was considered as a marker of autophagosome formation. However, more autophagosome formation could be because of either increased autophagosomes formation or decreased autolysosome degradation, which might result in serious cytotoxicity. In order to elucidate the autophagosome formation in Mst-$1^{-/-}$ mice, we used p62 to monitor autolysosome degradation, which is known to be degraded by autolysosome. At 7 days post-injury when the expression of LC3-II reached a peak, Mst-$1^{-/-}$ mice showed more LC3-II formation and less p62 accumulation than Mst-$1^{+/+}$ mice did, indicating more autophagosome formation and enhancement of autolysosome degradation in Mst-$1^{-/-}$ mice (Fig. 4d–f).

In a word, autophagy flux was disrupted after SCI, while Mst-1 deficiency could correct this disruption in a certain range via more autophagosome formation and enhancement of autolysosome degradation.

Mst-1 deficiency improves autophagy flux in motor neurons after SCI

Next, to confirm the enhancement of autophagy flux in spinal motor neurons, the expression of LC3-II and p62 were assessed by co-staining with ChAT. Similarly, our results provided more LC3-II formation and less p62 accumulation in Mst-$1^{-/-}$ than in Mst-$1^{+/+}$ spinal motor neurons, indicating both enhanced autophagosome formation and autolysosome

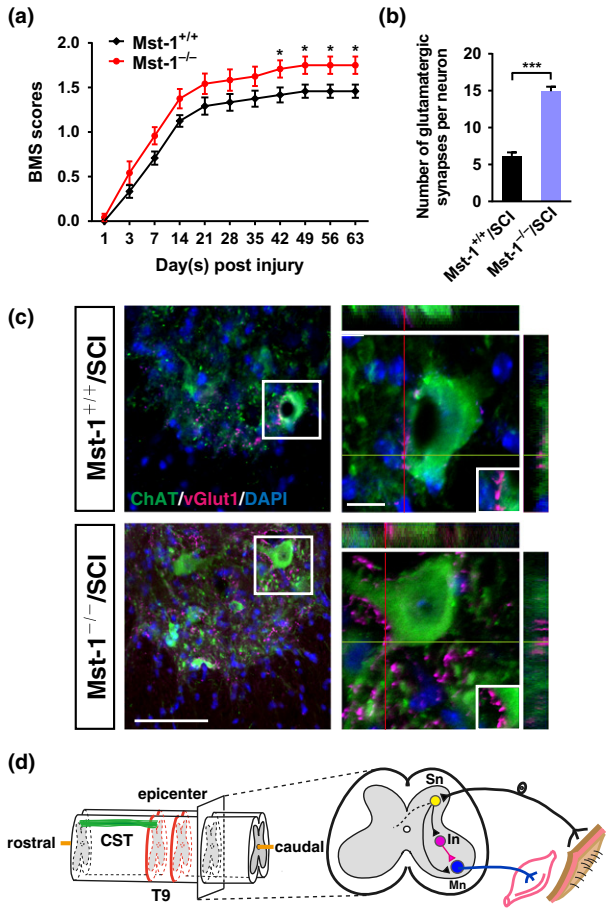

Fig. 3 Improvement of Basso mouse scale (BMS) scores and synapse reformation in Mst-1-deficient mice after spinal cord injury (SCI). (a) Timeline of the change in BMS scores in Mst-$1^{+/+}$ and Mst-$1^{-/-}$ mice after SCI. Data were presented as mean ± SEM of 15 independent experiments, each independent experiment including one mice per group. 42 days: $t = 2.748$, $p = 0.0394$; 49 days: $t = 3.247$, $p = 0.0127$; 56 days: $t = 2.998$, $p = 0.0249$; 63 days: $t = 2.998$, $p = 0.0249$. $^{*}p < 0.05$, two-way ANOVA followed by Fisher's least significant differences post-test (LSD). (b and c) Co-immunostaining (c) of vGlut1 and ChAT showing survived synapses between the glutamatergic terminals and motor neurons in Mst-$1^{+/+}$ and Mst-$1^{-/-}$ mice 9 weeks post-injury. Quantification of the glutamatergic synapses per neuron in each group was presented as mean ± SEM of five independent experiments, each independent experiment including one mice per group (b). $p = 0.0002$, $^{***}p < 0.001$, Student's t test. Scale bars, 100 μm (left), 20 μm (right). (d) Diagram showing the neuronal connection in spinal cord after T9 complete spinal transection.

degradation in spinal motor neurons of Mst-$1^{-/-}$ mice (Fig. 5a–d), which were consistent with the western blot results above (Fig. 4d–f). These results proved that, LC3 and p62 were accumulated in motor neurons and autophagy flux was disrupted after SCI, while Mst-1 deficiency could correct this disruption in a certain range by more autophagosome formation and enhancement of autolysosome degradation.

Taken together, we revealed that Mst-1 deficiency enhanced autophagy flux, through which injured spinal motor neurons adequately degraded toxic protein aggregates, and eventually, led to more motor neuron survival.

Autophagy flux is essential for Mst-1 deficiency to promote spinal motor neuron survival after SCI

To further investigate whether the neuroprotective effect of Mst-1 deficiency on spinal motor neuron survival after SCI was dependent on the enhancement of autophagy flux, Baf, a specific autophagy-lysosome pathway inhibitor was used to block autophagic flux (Klionsky *et al.* 2014). Immunostaining of ChAT revealed that the number of survived spinal motor neurons was decreased in both Mst-$1^{+/+}$ and Mst-$1^{-/-}$ groups with Baf treatment. However, the number of survived spinal motor neurons in Mst-$1^{+/+}$ group was less than in Mst-$1^{-/-}$ group after Baf treatment (Fig. 6a and b). These data revealed that the number of survived motor neurons was decreased with Baf treatment after SCI, suggesting autophagy flux was essential for Mst-1 deficiency to promote spinal motor neuron survival after SCI.

To further investigate the exact changes of autophagy-lysosome pathway with Baf treatment, LC3-II and p62 in the lesion area were detected with western blot and immunostaining. The increased level of p62 and LC3-II were detected in Baf group, indicating that Baf succeeded in suppressing the autolysosome degradation of autophagy-lysosome pathway. In addition, the Mst-$1^{-/-}$ group showed higher autolysosome degradation than in Mst-$1^{+/+}$ group, suggesting that Mst-1 deficiency could correct the suppression of autolysosome degradation with Baf treatment in a certain range (Fig. 6c–e). This might explain why there was less motor neuron loss in Mst-1-deficient mice with Baf treatment after SCI (Fig. 6a and b). Meanwhile, the expression tendencies of LC3-II and p62 in ChAT-positive motor neurons were consistent with the western blot tendencies above (Fig. 6f–i).

In summary, these results indicated that, autophagy flux was essential for Mst-1 deficiency to promote spinal motor neuron survival after SCI.

Discussion

Numerous neurological disorders are caused by the deposition of toxic protein aggregates. Inadequate protein degradation mechanisms, including abnormal autophagy and ubiquitin proteasome mechanisms, may lead to overloaded pathological stress and eventually neuron death (Shelkovnikova *et al.* 2012; Maejima *et al.* 2013). It is worth noting that, in SCI, the overloaded pathological stress around the lesion site leads to worse neuron survival after initial trauma. However, it is not clearly understood as to how these protein degradation mechanisms are related to SCI-induced pathological stress pathways.

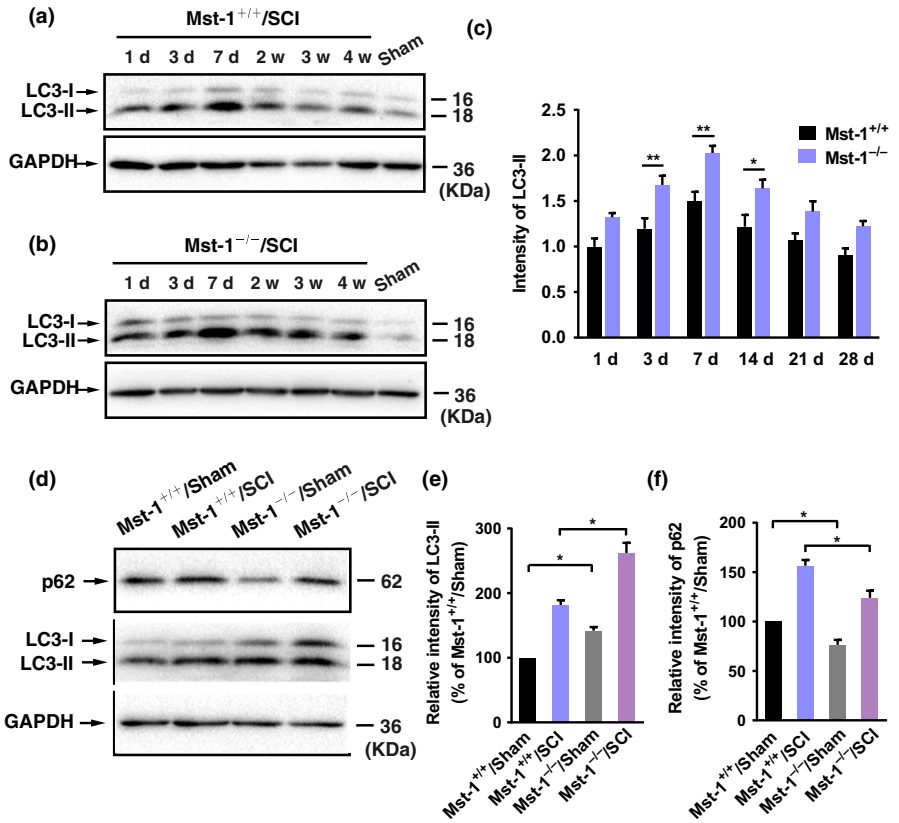

Fig. 4 Mst-1 deficiency promotes autophagy flux by more autophagosome formation and enhancement of autolysosome degradation. (a–c) Western blot analysis (a and b) and quantification (c) of LC3-II expression in the Mst-1$^{+/+}$ and Mst-1$^{-/-}$ lesion sites from day 1 to 4 weeks post-injury. Data were presented as mean ± SEM of three independent experiments, each independent experiment including three mice per group. 3 days: $t = 3.634$, $p = 0.0079$; 7 days: $t = 4.027$, $p = 0.0029$; 14 days: $t = 3.180$, $p = 0.0239$. $^{*}p < 0.05$ and $^{**}p < 0.01$, two-way ANOVA followed by Fisher's least significant differences post-test (LSD). (d–f) Western blot analysis (d) and quantification of LC3-II (e) and p62 (f) expression in the sham-operated and 7 days post-injury lesion area of the Mst-1$^{+/+}$ and Mst-1$^{-/-}$ mice. Data were presented as mean ± SEM of five independent experiments, each independent experiment including three mice per group. LC3-II intensity: Mst-1$^{+/+}$/Sham versus Mst-1$^{-/-}$/Sham, $t = 7.393$, $p = 0.0356$; Mst-1$^{+/+}$/spinal cord injury (SCI) versus Mst-1$^{-/-}$/SCI, $t = 7.802$, $p = 0.0321$. p62 intensity: Mst-1$^{+/+}$/Sham versus Mst-1$^{-/-}$/Sham, $t = 4.566$, $p = 0.0206$; Mst-1$^{+/+}$/SCI versus Mst-1$^{-/-}$/SCI, $t = 4.912$, $p = 0.0159$. $^{*}p < 0.05$, one-way ANOVA followed by Bonferroni's post-test.

As we know that, Hippo signaling pathway is considered to be essential for cell growth and survival. Recently, emerging evidence suggests that Hippo pathway is involved in the responses of pathological cellular stresses to maintain homeostasis in cellular and organic level (Mao *et al.* 2015). And accumulating evidence reveals that, as a component of the Hippo pathway, Mst-1 reacts to pathologically relevant stress and regulates cell death (Lehtinen *et al.* 2006; Yuan *et al.* 2009). In amyotrophic lateral sclerosis, Mst-1 may function as a key modulator of neurodegeneration in spinal motor neurons (Lee *et al.* 2013). Moreover, during cerebral ischemia–reperfusion injury, Mst-1 plays a crucial role in oxidative stress-induced neuron death (Zhao *et al.* 2016). However, its implication in SCI is very limited. Here, we demonstrated that genetic ablation of Mst-1 promotes SCI-induced motor neuron survival. However, although the Hippo/Mst-1 pathway can be stimulated by multiple types of cellular stress, including mechanical stress, DNA damage, and reactive oxygen species (Mao *et al.* 2015), it is still unknown how Mst-1 activation occurs during SCI-induced cellular stress (Hetz *et al.* 2009; Liu *et al.* 2010; Deng *et al.* 2013; Maejima *et al.* 2013; Li *et al.* 2014; Loers *et al.* 2014). Interestingly, consistent with previous report (Lee *et al.* 2013), we found the phosphorylation of Mst-1 at Thr183 was activated in SCI, and the activation was specific for motor neurons. Although oxidative-induced phosphorylation of Mst-1 at Y433 was activated in rat hippocampus neurons (Xiao *et al.* 2011), it was not induced in post-traumatic spinal motor neurons (data not shown). This might be because of the different mechanisms underlying the different phosphorylation sites, which are complex and remain to be elucidated.

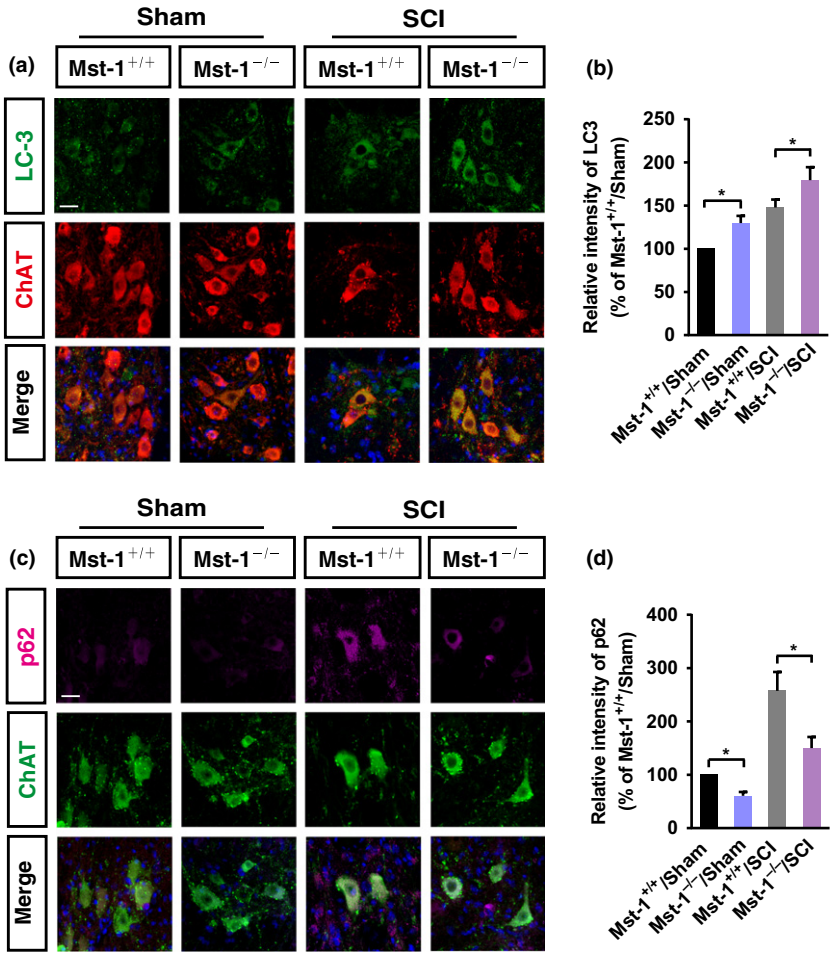

Fig. 5 Autophagy flux in motor neurons is enhanced by Mst-1 deficiency after spinal cord injury (SCI). (a and b) Immunostaining (a) and quantification (b) of LC3-II expression in ChAT-positive motor neurons in the sham-operated and 7 days post-injury lesion area of the Mst-$1^{+/+}$ and Mst-$1^{-/-}$ mice. Quantitative fluorescence intensity of LC3 was presented as mean ± SEM of more than 125 motor neurons from five independent experiments, each independent experiment including one mice per group. LC3-II intensity: Mst-$1^{+/+}$/Sham versus Mst-$1^{-/-}$/Sham, $t = 3.558$, $p = 0.0472$; Mst-$1^{+/+}$/SCI versus Mst-$1^{-/-}$/SCI, $t = 3.793$, $p = 0.0384$. $^*p < 0.05$, one-way ANOVA followed by Bonferroni's post-test. Scale bar, 20 μm. (c and d) Immunostaining (c) and quantification (d) of p62 expression in ChAT-positive motor neurons in the sham-operated and 7 days post-injury lesion area of the Mst-$1^{+/+}$ and Mst-$1^{-/-}$ mice. Quantitative fluorescence intensity of p62 was presented as mean ± SEM of more than 125 motor neurons from five independent experiments, each independent experiment including one mice per group. p62 intensity: Mst-$1^{+/+}$/Sham versus Mst-$1^{-/-}$/Sham, $t = 5.505$, $p = 0.0106$; Mst-$1^{+/+}$/SCI versus Mst-$1^{-/-}$/SCI, $t = 3.918$, $p = 0.0345$. $^*p < 0.05$, one-way ANOVA followed by Bonferroni's post-test. Scale bar, 20 μm.

Autophagy is an ancient catabolic process through which cells recycle toxic proteins and damaged organelles via an elaborate autophago-lysosomal pathway (Kroemer and Levine 2008; Dhingra and Kirshenbaum 2013; Lamb *et al.* 2013). Autophagy acts as an initial survival mechanism, which is rapidly induced during ischemia and neurotrauma (Galluzzi *et al.* 2016). In SCI, for instance, autophagy was thought to protect motor neurons against endoplasmic reticulum stress, and autophagy disruption could lead to endoplasmic reticulum-stress-induced neuronal apoptosis (Liu *et al.* 2015; Zhou *et al.* 2016). Another study showed that elevated autophagy inhibits cell death and protects spinal cord neurons during ischemia/reperfusion after SCI (Fan *et al.* 2014). Meanwhile, suppression of basal autophagy in neural cells caused neurodegenerative disease in mice (Hara *et al.* 2006). Despite an increasing attention to autophagy in SCI, whether autophagy promotes neuron survival or neuron death has not been figured out. For example, some studies indicated that enhanced autophagy leads to more neuron death (Kanno *et al.* 2011; Hao *et al.* 2013), while some other studies stated that autophagy enhancement promoted

injured neuron survival (Zhang *et al.* 2013; Tang *et al.* 2014; Goldshmit *et al.* 2015). This paradox might be partly owing to the intricacy balance of autophagy between neuron survival and neuron death, and partly owing to their neglect of autophagy flux.

Autophagy flux means the autophagy progress, from the formation of autophagosomes to its cargo delivery and degradation by the lysosomes, which plays a significant role in cellular homeostasis. Considering this progress, enhanced LC3 and autophagosomes do not always mean an increased autophagy flux. Either increased autophagosomes formation exceeding their degradation or decreased autolysosome degradation might result in autophagosomes accumulation. Therefore, it reminded us to examine autophagosomes formation as well as autolysosome degradation to ensure the state of autophagy flux (Del Re *et al.* 2014; Liang *et al.* 2014; Song *et al.* 2015; Hu *et al.* 2016). Our data revealed that, LC3 and p62 were enhanced after SCI, indicating that autolysosome degradation was suppressed and autophagy-lysosome pathway was disrupted, while Mst-1 deficiency could correct this disruption. Also, a research indicated that, upon early ischemia, activation of autophagy was protective, whereas late or delayed activation of autophagy was detrimental (Sciarretta *et al.* 2011). In Mst-1-deficient mice, it might be the enhanced autophagy flux at early stage after SCI, which ensured the clearance of damaged organelles and protein aggregates in injured motor neurons, leading to injured spinal motor neuron survival afterward.

It was difficult to investigate autophagy in spinal cord injury *in vitro*. Therefore, autophagy inhibitor was used *in vivo* to block autophagic flux in SCI mice. A small dose of Baf was used, because of its efficient blocking effect. And we combined i.p. with lesion site injection, to ensure the specificity and the least dosage of Baf treatment. Our data suggested that blocked autophagy flux accelerated the death of injured spinal motor neurons, indicating that unobstructed autophagy flux was essential for Mst-1 deficiency to promote spinal motor neuron survival. Therefore, these results might provide a possible explanation for the paradox above, as to why activated autophagy could lead to either beneficial or detrimental results, which is because enhanced autophagy does not mean enhanced autolysosome degradation, and an unobstructed autophagy flux may really be needed in neuron survival after SCI (Zhang *et al.* 2016). In addition, Baf treatment may lead to potential non-specific effects. Thus, to specifically block autophagy flux at genetic level is demanded in the future. Interestingly, some spinal motor neurons survived after Baf treatment in both Mst-$1^{-/-}$ and Mst-$1^{+/+}$ groups after SCI, which might indicate that autophagy was not the only way involved in the neuroprotective effect, other pathways might modulate motor neuronal survival as well.

Our results shown in this manuscript confirmed that Mst-1 deficiency promotes post-traumatic spinal motor neuron survival via enhancement of autophagy flux. However, the exact mechanism of Mst-1 in regulating autophagy is still unknown. Maejima *et al.* (2013) suggested that Mst-1 regulates autophagy via directly interacting between Mst-1 and Beclin1 rather than hippo signaling. They demonstrated that Mst-1 kinase becomes activated under cellular stress and phosphorylates Beclin1, which causes the loss of Beclin1–Atg14L–Vps34 complexes and impairs autophagy, resulting in protein aggregation and cell death (Maejima *et al.* 2013). However, we still cannot exclude the possibility of Mst-1 in regulating autophagy via Mst-1′s function in hippo signaling. Song *et al.* (2015) reported that Yes-associated protein (YAP) enhances autophagic flux to promote breast cancer cell survival in response to nutrient deprivation, and YAP-increased autolysosome degradation is TEA domain family transcription factors (TEAD)-dependent. As YAP's biological function is generally inhibited by Mst-1 in Hippo pathway, this finding suggested that the enhancement of autophagy flux via Mst-1 deficiency might be because of the function of YAP in Hippo signaling. In a word, Mst-1 deficiency might trigger sophisticated changes, and the mechanism of Mst-1 in regulating autophagy needs to be further investigated.

In summary, our findings revealed that p-Mst-1, the activation form of Mst-1, was specifically activated in post-traumatic spinal motor neurons. Furthermore, Mst-1 deficiency could correct the dysfunction of autophagy-lysosome pathway in injured motor neurons via more autophagosome formation and enhancement of autolysosome degradation, through which the adequate degradation of toxic protein aggregates reduced the motor neuron loss, and eventually, promoted synapse survival and improved behavioral outcome.

Author contributions

Y.L. supervised the project. M.Z. designed and performed the experiment. M.Z., W.T., and Z.Y. analyzed the data. M.Z. wrote the manuscript. M.Z. and Y.L. edited the manuscript.

Acknowledgments and conflict of interest disclosure

This study was supported by grants from the National Natural Science Foundation of China (numbers 81330026, 81771330, 31271259), the National Key Basic Research Development Program of the Ministry of Science and Technology of China (973 Program) (2013CB945604), and A Project Funded by the Priority Academic Program Development of Jiangsu Higher Education Institutions. The authors declare no competing financial interests.

All experiments were conducted in compliance with the ARRIVE guidelines.

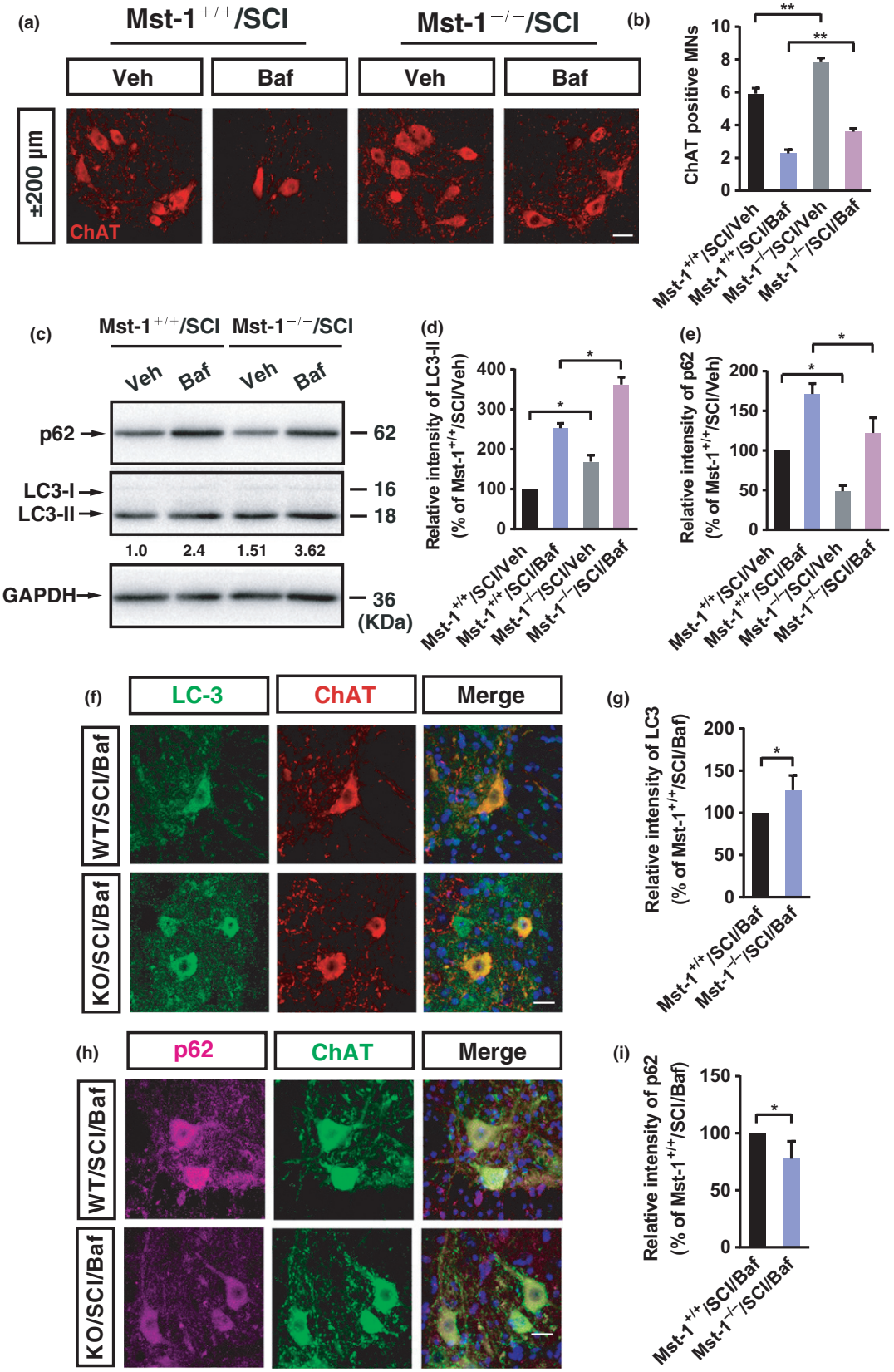
(a)
Mst-1+/+/SCI
Mst-1−/−/SCI
Veh
Baf
Veh
Baf
±200 μm
ChAT
(b)
ChAT positive MNs
Mst-1+/+/SCI/Veh
Mst-1+/+/SCI/Baf
Mst-1−/−/SCI/Veh
Mst-1−/−/SCI/Baf
(c)
Mst-1+/+/SCI
Mst-1−/−/SCI
Veh
Baf
Veh
Baf
p62
LC3-I
LC3-II
62
16
18
1.0
2.4
1.51
3.62
GAPDH
36
(KDa)
(d)
Relative intensity of LC3-II
(% of Mst-1+/+/SCI/Veh)
(e)
Relative intensity of p62
(% of Mst-1+/+/SCI/Veh)
(f)
LC-3
ChAT
Merge
WT/SCI/Baf
KO/SCI/Baf
(g)
Relative intensity of LC3
(% of Mst-1+/+/SCI/Baf)
(h)
p62
ChAT
Merge
WT/SCI/Baf
KO/SCI/Baf
(i)
Relative intensity of p62
(% of Mst-1+/+/SCI/Baf)

Fig. 6 Autophagy flux enhanced by Mst-1 deficiency was crucial to attenuate the death of spinal motor neurons after spinal cord injury (SCI). (a and b) Immunostaining (a) and quantification (b) of ChAT-positive motor neurons in the Mst-$1^{+/+}$ and Mst-$1^{-/-}$ mice 4 weeks post-injury after Baf treatment. Data were presented as mean ± SEM of five independent experiments, each independent experiment including one mice per group. Mst-$1^{+/+}$/SCI/Veh versus Mst-$1^{-/-}$/SCI/Veh, $t = 7.945$, $p = 0.0027$; Mst-$1^{+/+}$/SCI/Baf versus Mst-$1^{-/-}$/SCI/Baf, $t = 8.124$, $p = 0.0025$. $^{**}p < 0.01$, one-way ANOVA followed by Bonferroni's post-test. Scale bar, 20 μm. (c–e) Western blot analysis (c) and quantification of LC3-II (d) and p62 (e) expression in the lesion area of the Mst-$1^{+/+}$ and Mst-$1^{-/-}$ mice 7 days post-injury after Baf treatment. Data were presented as mean ± SEM of five independent experiments, each independent experiment including three mice per group. LC3-II intensity: Mst-$1^{+/+}$/SCI/Veh versus Mst-$1^{-/-}$/SCI/Veh, $t = 7.211$, $p = 0.0374$; Mst-$1^{+/+}$/SCI/Baf versus Mst-$1^{-/-}$/SCI/Baf, $t = 6.806$, $p = 0.0418$. p62 intensity: Mst-$1^{+/+}$/SCI/Veh versus Mst-$1^{-/-}$/SCI/Veh, $t = 12.38$, $p = 0.0129$; Mst-$1^{+/+}$/SCI/Baf versus Mst-$1^{-/-}$/SCI/Baf, $t = 11.03$, $p = 0.0162$. $^{*}p < 0.05$, one-way ANOVA followed by Bonferroni's post-test. (f and g) Immunostaining (f) and quantification (g) of LC3-II expression in ChAT-positive motor neurons in the lesion area of the Mst-$1^{+/+}$ and Mst-$1^{-/-}$ mice 7 days post-injury after Baf treatment. Quantitative fluorescence intensity of LC3-II was presented as mean ± SEM of more than 125 motor neurons from five independent experiments, each independent experiment including one mice per group. $p = 0.0255$, $^{*}p < 0.05$, Student's t test. Scale bar, 20 μm. (h and i) Immunostaining (h) and quantification (i) of p62 expression in ChAT-positive motor neurons in the lesion area of the Mst-$1^{+/+}$ and Mst-$1^{-/-}$ mice 7 days post-injury after Baf treatment. Quantitative fluorescence intensity of p62 was presented as mean ± SEM of more than 125 motor neurons from five independent experiments, each independent experiment including one mice per group. $p = 0.0306$, $^{*}p < 0.05$, Student's t test. Scale bar, 20 μm.

Supporting information

Additional Supporting Information may be found online in the supporting information tab for this article:

Figure S1. Up-regulation of p-Mst-1 in spinal motor neurons and undetectable change in the number of neurons in dorsal and intermediate zone of Mst-$1^{+/+}$ and Mst-$1^{-/-}$ spinal cord after SCI.

Figure S2. Mst-1 deficiency promotes survival of injured motor neuron after spinal crush injury.

References

Cordaro M., Paterniti I., Siracusa R., Impellizzeri D., Esposito E. and Cuzzocrea S. (2017) KU0063794, a dual mTORC1 and mTORC2 inhibitor, reduces neural tissue damage and locomotor impairment after spinal cord injury in mice. *Mol. Neurobiol.* **54**, 2415–2427.

Del Re D. P., Matsuda T., Zhai P., Maejima Y., Jain M. R., Liu T., Li H., Hsu C. P. and Sadoshima J. (2014) Mst1 promotes cardiac myocyte apoptosis through phosphorylation and inhibition of Bcl-xL. *Mol. Cell* **54**, 639–650.

Deng L. X., Deng P., Ruan Y., Xu Z. C., Liu N. K., Wen X., Smith G. M. and Xu X. M. (2013) A novel growth-promoting pathway formed by GDNF-overexpressing Schwann cells promotes propriospinal axonal regeneration, synapse formation, and partial recovery of function after spinal cord injury. *J. Neurosci.* **33**, 5655–5667.

Dhingra R. and Kirshenbaum L. A. (2013) Mst-1 switches between cardiac cell life and death. *Nat. Med.* **19**, 1367–1368.

Dong Y., Du X., Ye J., Han M., Xu T., Zhuang Y. and Tao W. (2009) A cell-intrinsic role for Mst1 in regulating thymocyte egress. *J. Immunol.* **183**, 3865–3872.

Fan J., Zhang Z., Chao X., Gu J., Cai W., Zhou W., Yin G. and Li Q. (2014) Ischemic preconditioning enhances autophagy but suppresses autophagic cell death in rat spinal neurons following ischemia-reperfusion. *Brain Res.* **1562**, 76–86.

Galluzzi L., Bravo-San Pedro J. M., Blomgren K. and Kroemer G. (2016) Autophagy in acute brain injury. *Nat. Rev. Neurosci.* **17**, 467–484.

Goldshmit Y., Kanner S., Zacs M., Frisca F., Pinto A. R., Currie P. D. and Pinkas-Kramarski R. (2015) Rapamycin increases neuronal survival, reduces inflammation and astrocyte proliferation after spinal cord injury. *Mol. Cell Neurosci.* **68**, 82–91.

Hao H. H., Wang L., Guo Z. J. *et al.* (2013) Valproic acid reduces autophagy and promotes functional recovery after spinal cord injury in rats. *Neurosci. Bull.* **29**, 484–492.

Hara T., Nakamura K., Matsui M. *et al.* (2006) Suppression of basal autophagy in neural cells causes neurodegenerative disease in mice. *Nature* **441**, 885–889.

Hetz C., Thielen P., Matus S. *et al.* (2009) XBP-1 deficiency in the nervous system protects against amyotrophic lateral sclerosis by increasing autophagy. *Genes Dev.* **23**, 2294–2306.

Hu J., Man W., Shen M. *et al.* (2016) Luteolin alleviates post-infarction cardiac dysfunction by up-regulating autophagy through Mst1 inhibition. *J. Cell Mol. Med.* **20**, 147–156.

Huang Z., Gao Y., Sun Y., Zhang C., Yin Y., Shimoda Y., Watanabe K. and Liu Y. (2016) NB-3 signaling mediates the cross-talk between post-traumatic spinal axons and scar-forming cells. *EMBO J.* **35**, 1745–1765.

Kanno H., Ozawa H., Sekiguchi A., Yamaya S. and Itoi E. (2011) Induction of autophagy and autophagic cell death in damaged neural tissue after acute spinal cord injury in mice. *Spine* **36**, E1427–E1434.

Klionsky D. J., Elazar Z., Seglen P. O. and Rubinsztein D. C. (2014) Does bafilomycin A1block the fusion of autophagosomes with lysosomes? *Autophagy* **4**, 849–850.

Kroemer G. and Levine B. (2008) Autophagic cell death: the story of a misnomer, Nature reviews Molecular cell biology (Nat Rev Mol Cell Biol), **9**, 1004–1010.

Lamb C. A., Yoshimori T. and Tooze S. A. (2013) The autophagosome: origins unknown, biogenesis complex. *Nat. Rev. Mol. Cell Biol.* **14**, 759–774.

Lee J. K., Shin J. H., Hwang S. G., Gwag B. J., McKee A. C., Lee J., Kowall N. W., Ryu H., Lim D. S. and Choi E. J. (2013) MST1 functions as a key modulator of neurodegeneration in a mouse model of ALS. *PNAS*, **110**, 12066–12071.

Lehtinen M. K., Yuan Z., Boag P. R. *et al.* (2006) A conserved MST-FOXO signaling pathway mediates oxidative-stress responses and extends life span. *Cell* **125**, 987–1001.

Li K., Nicaise C., Sannie D. *et al.* (2014) Overexpression of the astrocyte glutamate transporter GLT1 exacerbates phrenic motor neuron degeneration, diaphragm compromise, and forelimb motor dysfunction following cervical contusion spinal cord injury. *J. Neurosci.* **34**, 7622–7638.

Li H. T., Zhao X. Z., Zhang X. R., Li G., Jia Z. Q., Sun P., Wang J. Q., Fan Z. K. and Lv G. (2016) Exendin-4 enhances motor function recovery via promotion of autophagy and inhibition of neuronal

apoptosis after spinal cord injury in rats. *Mol. Neurobiol.* **53**, 4073–4082.

Liang N., Zhang C., Dill P. *et al.* (2014) Regulation of YAP by mTOR and autophagy reveals a therapeutic target of tuberous sclerosis complex. *J. Exp. Med.* **211**, 2249–2263.

Lipinski M. M., Wu J., Faden A. I. and Sarkar C. (2015) Function and mechanisms of autophagy in brain and spinal cord trauma. *Antioxid. Redox Signal.* **23**, 565–577.

Liu Y., Wang X., Lu C. C., Kerman R., Steward O., Xu X. M. and Zou Y. (2008) Repulsive Wnt signaling inhibits axon regeneration after CNS injury. *J. Neurosci.* **28**, 8376–8382.

Liu K., Lu Y., Lee J. K. *et al.* (2010) PTEN deletion enhances the regenerative ability of adult corticospinal neurons. *Nat. Neurosci.* **13**, 1075–1081.

Liu S., Sarkar C., Dinizo M., Faden A. I., Koh E. Y., Lipinski M. M. and Wu J. (2015) Disrupted autophagy after spinal cord injury is associated with ER stress and neuronal cell death. *Cell Death Dis.* **6**, e1582.

Loers G., Cui Y. F., Neumaier I., Schachner M. and Skerra A. (2014) A Fab fragment directed against the neural cell adhesion molecule L1 enhances functional recovery after injury of the adult mouse spinal cord. *Biochem. J.* **460**, 437–446.

Maejima Y., Kyoi S., Zhai P. *et al.* (2013) Mst1 inhibits autophagy by promoting the interaction between Beclin1 and Bcl-2. *Nat. Med.* **19**, 1478–1488.

Mao B., Gao Y., Bai Y. and Yuan Z. (2015) Hippo signaling in stress response and homeostasis maintenance. *Acta Biochim. Biophys. Sin.* **47**, 2–9.

Michele Basso D., Fisher Lesley C., Anderson Aileen J., Jakeman Lyn B., Mctigue Dana M. and Popovich P. G. (2006) Basso mouse scale for locomotion detects differences in recovery after spinal cord injury in five common mouse strains. *J. Neurotrauma* **23**, 635–659.

Ravikumar B., Vacher C., Berger Z. *et al.* (2004) Inhibition of mTOR induces autophagy and reduces toxicity of polyglutamine expansions in fly and mouse models of Huntington disease. *Nat. Genet.* **36**, 585–595.

Sciarretta S., Hariharan N., Monden Y., Zablocki D. and Sadoshima J. (2011) Is autophagy in response to ischemia and reperfusion protective or detrimental for the heart? *Pediatr. Cardiol.* **32**, 275–281.

Sekiguchi A., Kanno H., Ozawa H., Yamaya S. and Itoi E. (2012) Rapamycin promotes autophagy and reduces neural tissue damage and locomotor impairment after spinal cord injury in mice. *J. Neurotrauma* **29**, 946–956.

Shelkovnikova T. A., Kulikova A. A., Tsvetkov P. O., Peters O., Bachurin S. O., Buchman V. L. and Ninkina N. N. (2012) Proteinopathies, neurodegenerative disorders with protein aggregation-based pathology. *Mol. Biol.* **46**, 362–374.

Smith C. M., Chen Y., Sullivan M. L., Kochanek P. M. and Clark R. S. (2011) Autophagy in acute brain injury: feast, famine, or folly? *Neurobiol. Dis.* **43**, 52–59.

Song Q., Mao B., Cheng J., Gao Y., Jiang K., Chen J., Yuan Z. and Meng S. (2015) YAP enhances autophagic flux to promote breast cancer cell survival in response to nutrient deprivation. *PLoS ONE* **10**, 1–17.

Tang P., Hou H., Zhang L., Lan X., Mao Z., Liu D., He C., Du H. and Zhang L. (2014) Autophagy reduces neuronal damage and promotes locomotor recovery via inhibition of apoptosis after spinal cord injury in rats. *Mol. Neurobiol.* **49**, 276–287.

Viscomi M. T. and Molinari M. (2014) Remote neurodegeneration: multiple actors for one play. *Mol. Neurobiol.* **50**, 368–389.

Watson C., Paxinos G. and Kayalioglu G. (2009) *The Spinal Cord: A Christopher and Dana Reeve Foundation Text and Atlas*. Academic Press, San Diego.

Xiao L., Chen D., Hu P. *et al.* (2011) The c-Abl-MST1 signaling pathway mediates oxidative stress-induced neuronal cell death. *J. Neurosci.* **31**, 9611–9619.

Yuan Z., Lehtinen M. K., Merlo P., Villen J., Gygi S. and Bonni A. (2009) Regulation of neuronal cell death by MST1-FOXO1 signaling. *J. Biol. Chem.* **284**, 11285–11292.

Yuan N., Song L., Zhang S. *et al.* (2015) Bafilomycin A1 targets both autophagy and apoptosis pathways in pediatric B-cell acute lymphoblastic leukemia. *Haematologica* **100**, 345–356.

Zhang H. Y., Wang Z. G., Wu F. Z. *et al.* (2013) Regulation of autophagy and ubiquitinated protein accumulation by bFGF promotes functional recovery and neural protection in a rat model of spinal cord injury. *Mol. Neurobiol.* **48**, 452–464.

Zhang D., Xuan J., Zheng B. B. *et al.* (2017) Metformin improves functional recovery after spinal cord injury via autophagy flux stimulation. *Mol. Neurobiol.* **54**, 3327–3341.

Zhao S., Yin J., Zhou L. *et al.* (2016) Hippo/MST1 signaling mediates microglial activation following acute cerebral ischemia-reperfusion injury. *Brain Behav. Immun.* **55**, 236–248.

Zhou Y., Zhang H., Zheng B. *et al.* (2016) Retinoic acid induced-autophagic flux inhibits ER-stress dependent apoptosis and prevents disruption of blood-spinal cord barrier after spinal cord injury. *Inter. J. Biol. Sci.* **12**, 87–99.

Zou Y. (2013) An update on spinal cord injury research. *Neurosci. Bull.* **29**, 399–401.